The classical mutual information in mean-field spin glass models

Vincenzo Alba,[1] Stephen Inglis,[2] and Lode Pollet[2]

[1]*International School for Advanced Studies (SISSA), Via Bonomea 265, 34136, Trieste, Italy, INFN, Sezione di Trieste*
[2]*Department of Physics and Arnold Sommerfeld Center for Theoretical Physics, Ludwig-Maximilians-Universität München, D-80333 München, Germany*

(Dated: May 27, 2015)

We investigate the *classical* Rényi entropy S_n and the associated mutual information $\mathcal{I}_n$ in the Sherrington-Kirkpatrick (S-K) model, which is the paradigm model of mean-field spin glasses. We use both classical Monte Carlo simulations and analytical tools. First, we investigate the S-K model on the n-sheets booklet. This is obtained by gluing together n independent copies of the model, and it is the main ingredient to construct entaglement-related quantities. We find that at low temperature the S-K model is in a glassy phase, whereas at high temperature it exhibits paramagnetic behavior. Interestingly, the critical temperature of the paramagnetic-glassy transition depends in a non-trivial way on the geometry of the booklet. At high-temperatures we provide the exact solution of the model exploiting the replica symmetry. This is the permutation symmetry among the fictitious replicas that are used in the replica trick to perform disorder averages. In the low-temperature glassy phase the replica symmetry has to be broken. Using a simple generalization of the celebrated Parisi solution, we provide approximated results for thermodynamic quantities and for S_n and $\mathcal{I}_n$. Finally, we show that both S_n and $\mathcal{I}_n$ exhibit a volume law in the whole phase diagram. Their densities S_n/N and $\mathcal{I}_n/N$ are finite and smooth function of the temperature, in the thermodynamic limit. In contrast with local spin models, $\mathcal{I}_n/N$ does not exhibit any crossing for different system sizes at the critical point.

I. INTRODUCTION

Besides being ubiquitous in nature, disorder leads to several intriguing physical phenomena. Arguably, *spin glasses* provide one of the most striking examples. While at any finite temperature disorder prevents the usual magnetic ordering, at low-enough temperatures these systems display a new and exotic type of "order". In the past decades an intense theoretical effort has been devoted to characterizing this spin glass order, the nature of the paramagnetic-glassy transition, and that of the associated order parameter[8,9,12,28,53].

All these issues have been thoroughly addressed in the Sherrington-Kirkpatrick (S-K) model[20,21], which is exactly solvable. The S-K model is a *classical* Ising model on the fully-connected graph of N sites, with quenched random interactions. Its hamiltonian reads

$$\mathcal{H} = -\sum_{1\leq i<j\leq N} J_{ij} S_i S_j - h \sum_{1\leq i\leq N} S_i. \qquad (1)$$

Here $S_i = \pm 1$ are classical Ising spins, h is an external magnetic field, and J_{ij} are uncorrelated (from site to site) random variables. The S-K model hosts a low-temperature glassy phase, which is separated from a high-temperature paramagnetic one by a second order phase transition. In contrast with the mean-field nature of Eq. (1), the solution of the S-K model has been a mathematical challenge. Although it was proposed as an ansatz by Parisi[22] more than thirthy years ago, its rigourous proof was obtained only recently[48]. Moreover, the solution exhibits several intricate features, such as lack of self-averaging[56], ultrametricity[27,50], and replica symmetry breaking[12,53]. The last refers to the breaking of the permutation symmetry among the fictitious replicas of the system, which in the standard replica trick[41] are used to perform disorder averages. Finally, although the applicability of the S-K model to describe realistic spin glasses is still highly debated[31–33], we should mention that there are recent proposals on how to realize this model in cold-atomic gases[34,36], or in laser systems[35].

In the last decade entanglement-related quantities have emerged as valuable tools to understand the physics of complex systems[1–4], both classical and quantum. For instance, at a conformally invariant critical point entanglement measures contain universal information about the underlying conformal field theory (CFT), such as the central charge[5–7,51]. For classical spin models a lot of attention has been focused on the *classical* Rényi entropy[29,30]. Given a bipartition of the system into two complementary subregions A and B, the classical Rényi entropy $S_n(A)$ (with $n \in \mathbb{N}$) is defined as

$$S_n(A) \equiv \frac{1}{1-n} \log\Big(\sum_{i_A \in \mathcal{C}_A} p_{i_A}^n\Big).i \qquad (2)$$

Here $\mathcal{C}_A$ denotes the set of all the possible spin configurations in part A, whereas p_{i_A} is the probability of the configuration i_A. Alternatively, $S_n(A)$ can be obtained from the partition function of the model on an *ad hoc* defined "booklet" geometry (see section II for its precise definition). This consists of n independent and identical replicas (the booklet "sheets") of the model. Notice that these *physical* replicas are different from the *fictitious* ones used to perform the disorder average. Each sheet is divided into two parts A and B, containing N_A and N_B spins, respectively. The spins in part A of different sheets are constrained to be equal. It is convenient to introduce the aspect ratio $0 \leq \omega \leq 1$ as

$$\omega \equiv \frac{N_A}{N}. \qquad (3)$$

Clearly, Eq. (2) can be extended to quantum systems[43–47,52] by interpreting p_{i_A} as the probability of finding part A in the *quantum* configuration i_A. From $S_n(A)$, one defines the classical mutual information $\mathcal{I}_n(A,B)$ as

$$\mathcal{I}_n(A,B) \equiv S_n(A) + S_n(B) - S_n(A\cup B). \qquad (4)$$

For local models $\mathcal{I}_n$ obeys the area law[54] $\mathcal{I}_n(A) \propto \ell$, with ℓ being the length of the boundary between A and B. Remarkably, for different ℓ, the ratio $\mathcal{I}_n/\ell$ exhibits a crossing at a second order phase transition[30], and it can be used as a diagnostic tool for critical behaviors. For conformally invariant critical models more universal information can be extracted from the subleading contributions, i.e., the corrections to the area law, of $\mathcal{I}_n$[29].

Recently, the study of the interplay between disorder and entanglement became a fruitful research area[55]. However, the behavior of entanglement-related quantities in glassy phases, and at glassy critical points, has not been explored yet. Here we investigate both the classical Rényi entropy $S_n(A)$ and the mutual information $\mathcal{I}_n$ in the S-K model, using classical Monte Carlo simulations and analytical tools. We often restrict ourselves to the case with $n = 2$. As usual in disordered system, we focus on disorder-averaged quantities, considering $[S_n]$ and $[\mathcal{I}_n]$, with the brackets $[\cdot]$ denoting the average over different realizations of J_{ij} in Eq. (1).

We start discussing the thermodynamic phase diagram of the S-K model on the n-sheets booklet, as a function of temperature, and the aspect ratio ω (cf. Eq. (3)). We find that for any ω the S-K model exhibits a low-temperature glassy phase, which is divided by the standard paramagnetic one at high temperatures by a critical point. Surprisingly, the critical temperature exhibits a non-trivial dependence on ω that we are able to determine analytically. In the high-temperature region, for any fixed ω, the permutational symmetry among the replicas, both the physical and the fictitious ones, is preserved. This allows us to provide an exact analytic expression for the free energy of the model and several derived quantities, such as the internal energy. We check our result against Monte Carlo simulations, finding perfect agreement. Oppositely, we provide both numerical and analytical evidence that in the low-temperature phase, for any ω, the replica symmetry has to be broken. Specifically, we numerically observe that the replica-symmetric (RS) result for the internal energy is systematically lower than the Monte Carlo data, as in the standard S-K model[20,21]. This discrepancy becomes larger upon lowering the temperature.

Inspired by the Parisi scheme[25], we devise a systematic way of breaking the replica symmetry in successive steps. Precisely, our scheme breaks only the symmetry among the fictitious replicas, preserving that among the physical ones. Although this appears natural, we are not able to provide a rigourous proof that this is the correct symmetry breaking pattern. In particular, we cannot exclude that the symmetry among the physical replicas has to be broken. As a consequence, our scheme should be regarded as an approximation, and not as an exact solution. Finally, we should mention that we restrict ourselves to the one-level replica symmetry breaking (1-RSB). This, however, is a minor limitation because, in principle, it is possible to implement in our ansatz the full breaking of the replica symmetry (∞-RSB). Surprisingly, we numerically observe that the 1-RSB approximation for the internal energy is in excellent agreement with the Monte Carlo data for $\beta \lesssim 3$, whereas the RS approximation fails already at $\beta \approx 1$. This suggests that the 1-RSB ansatz captures correctly some aspects of the replica symmetry breaking.

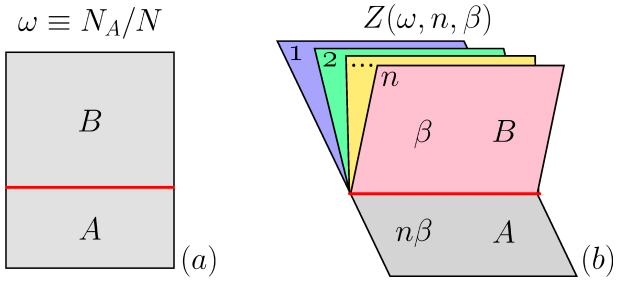

FIG. 1. The booklet geometry considered in this work. (a) The single sheet ("page") of the booklet: The N spins living on the sheet are divided into two groups A and B, containing N_A and N_B spins, respectively. Here $\omega \equiv N_A/N$ is the booklet ratio. (b) The n sheets are glued together to form the booklet. The spins in part B of the booklet pages are at inverse temperature β. The spins in part A are identified (see Eq. (11)). As a consequence, the effective temperature in part A is $n\beta$. $Z(\omega, n, \beta)$ denotes the partition function of the S-K model on the booklet.

This scenario, and, in particular, the effects of the replica symmetry breaking, are reflected in the behavior of $[S_2]$ and $[\mathcal{I}_2]$. First, since $[S_2]$ exhibits the volume law behavior $[S_2] \propto N$, we consider its density $[S_2]/N$. For finite-size systems, and for any ω, we find that $[S_2]/N$ exhibits a maximum at infinite temperature, and it is a monotonically decreasing function of the temperature. More specifically, the Monte Carlo data suggest a vanishing behavior in the zero-temperature limit. Moreover, the finite-size corrections are negligible at high temperatures, whereas they increase upon lowering the temperature. A standard finite-size scaling analysis shows that in the thermodynamic limit $[S_2]/N$ is finite and smooth as a function of β and ω, in the whole phase diagram. In the paramagnetic phase we are able to calculate the functional form of $[S_2]$, using the replica-symmetric approximation. This perfectly matches the Monte Carlo data. At low temperatures deviations from the replica-symmetric result are observed, reflecting the replica symmetry breaking. Remarkably, we observe that the one-step replica symmetry breaking (1-RSB) approximation $S_2^{1\text{-}RSB}/N$ is in full agreement with the Monte Carlo data for $\beta \lesssim 3$, confirming what is observed for the internal energy.

Finally, we consider the Rényi mutual information $[\mathcal{I}_2]$. This obeys a volume law for any β and ω, in sharp contrast with local spin models, where an area law is observed[54]. The mutual information density $[\mathcal{I}_2]/N$ vanishes in both the infinite-temperature and the zero-temperature limits, for any ω. Surprisingly, for different sizes $\mathcal{I}_2/N$ does not exhibit any crossing at the paramagnetic-glassy transition, in striking contrast with local spin models[30]. In the thermodynamic limit $[\mathcal{I}_2]/N$ is finite and smooth (as a function of β) in the whole phase diagram. Interestingly, for any ω, $\mathcal{I}_2/N$ exhibits a maximum for $\beta \approx 1$. However, the position of this maximum is not simply related to paramagnetic-glassy transition. Finally, at high temperature $[\mathcal{I}_2]/N$ is fully described analytically within the replica symmetric approximation, whereas at low temperatures one has to include the effects of the replica

symmetry breaking. Similar to $[S_2]$, we observe that the 1-RSB approximation for $[\mathcal{I})_2]/N$, is in good agreement with the Monte Carlo data for $\beta \approx 3$.

The Article is organized as follows. In section II we introduce the classical Rényi entropy and the mutual information, reviewing their representation in terms of the booklet partition functions. In section III we present the structure of the the solution of the S-K model on the booklet. Specifically, we discuss the replica trick, which is used to perform disorder averages, and the saddle point approximation in the thermodynamic limit . Section IV is concerned with the replica-symmetric (RS) approximation. In subsection IV A we focus on the high-temperature region where this approximation becomes exact. In subsection IV B we discuss the RS ansatz in the low-temperature region. Section V is devoted to presenting the one-step replica symmetry breaking (1-RSB) approximation. In section VI we check the validity of both the RS and the 1-RSB approximations against Monte Carlo data. Section VII and VIII present our results for the classical Rényi entropy and the mutual information, respectively. Finally, we conclude in section IX.

II. THE BOOKLET CONSTRUCTION & AND THE CLASSICAL MUTUAL INFORMATION

Given a generic *classical* spin model at inverse temperature β, the Rényi mutual information $\mathcal{I}_n(A,B,\beta)$ (with $n \in \mathbb{N}$) is defined as[29,30]

$$\mathcal{I}_n(A,B,\beta) \equiv \frac{1}{1-n}\log\left(\frac{Z(A,n,\beta)Z(B,n,\beta)}{Z(\beta)^n Z(n\beta)}\right). \quad (5)$$

Here $Z(A,n,\beta)$ is the partition function of the model on the so-called n-sheet booklet, whereas $Z(\beta)$ and $Z(n\beta)$ are the partition functions on a the plane (a single sheet) at inverse temperatures β and $n\beta$, respectively. The booklet geometry is illustrated in Figure 1. The sheet is divided into two parts A and B (cf. Figure 1 (a)). Then n copies of the system ("sheets") are "glued" together to form the booklet. The spins in part A of different sheets are identified (cf. Figure 1 (b)). Notice that a similar construction[49] plays an important role in the mathematical proof of the Parisi ansats. While spins in B are at inverse temperature β, the ones in A are at the effective temperature $n\beta$. The definition of $Z(B,n\beta)$ is obtained by exchanging A and B. Alternatively, $\mathcal{I}_n$ can be rewritten as

$$\mathcal{I}_n(A,B,\beta) = S_n(A) + S_n(B) - S_n(A\cup B), \quad (6)$$

where $S_n(X)$ is the "booklet" classical Rényi entropy

$$S_n(X) \equiv \frac{1}{1-n}\log\left(\frac{Z(X,n,\beta)}{Z^n(\beta)}\right). \quad (7)$$

Notice that $S_n(X)$ corresponds to $S_n(X) \equiv 1/(n-1)\log(F(X,n,\beta)) - n\log(F(\beta))$, where $F(X,n,\beta) \equiv \log(Z(\beta))$ and $F(\beta) \equiv \log(Z(X,n,\beta))$ are related (apart from a factor β) to the free energy of the model on the booklet and on the plane, respectively. Since here we focus on the effects of the disorder, we consider the disorder-averaged mutual information $[\mathcal{I}_n]$

$$[\mathcal{I}_n(A,B,\beta)] = [S_n(A)] + [S_n(B)] - [S_n(A\cup B)], \quad (8)$$

where the square brackets $[\cdot]$ denote the average over different disorder realizations (cf. section III). Notice that $[\mathcal{I}_n]$ is directly obtained from the so-called quenched averaged free energy $[F(X,n,\beta)]$, which is usually considered in disordered systems[41].

For clean (i.e., without disorder) *local* spin models $\mathcal{I}_n$ obeys the boundary law

$$\mathcal{I}_n(A,B,\beta) = \alpha_n \ell + \mathcal{G}_n + \gamma_n, \quad (9)$$

with ℓ the length of the boundary between A and B, and α_n, γ_n two non-universal constants. Here $\mathcal{G}_n$ is the so-called geometric mutual information[29]. Interestingly, for critical systems $\mathcal{G}_n$ depends only on the geometry of A and B, and it is universal. In particular, for conformally invariant models $\mathcal{G}_n$ can be calculated using standard methods of conformal field theory (CFT), and it allows to numerically extract universal information about the CFT, such as the central charge[29]. Remarkably, there is numerical evidence that $\mathcal{I}_n/\ell$ exhibits a crossing for different system sizes at a second order phase transition, implying that it can be used as a diagnostic tool to detect phase transitions[30].

III. THE SHERRINGTON-KIRKPATRICK (S-K) MODEL ON THE BOOKLET

Here we introduce the Sherrington-Kirkpatrick (S-K) model on the booklet (see Fig. 1). In particular, in subsection III A we define the model and its partition function. In subsection III B we discuss the replicated booklet construction that is used to calculate the disorder-averaged free energy $[F(\omega,n,\beta)]$. In III C we consider the thermodynamic limit, using the saddle point approximation. We also introduce the overlap tensor, which contains all the information about the thermodynamic behavior of the model. The analytical formula for the replicated partition function (Eq. (22)) of the S-K the model, and the saddle point equations (Eqs. (24)) for the overlap tensor are the main results of this section.

A. The model and its partition function

The Sherrington-Kirkpatrick (S-K) model[20,21] on the n-sheets booklet (cf. Figure 1) is defined by the Hamiltonian

$$\mathcal{H} = -\sum_{r=1}^{n}\left\{\sum_{i<j} J_{ij} S_i^{(r)} S_j^{(r)} - h\sum_{i=1}^{N} S_i^{(r)}\right\}. \quad (10)$$

Here $S_i^{(r)} = \pm 1$ are classical Ising spins, $r \in [1,n]$ labels the different sheets ("pages") of the booklet, $i \in [1,N]$ denotes the sites on each sheet, J_{ij} is the interaction strength, and h is an external magnetic field. Here we choose $h = 0$. The total

number of spins in the booklet is nN. The first sum inside the brackets in Eq. (10) is over all the $N(N-1)/2$ pairs of spins in each sheet. Spins on different sheets do not interact. In each "page" all the sites are divided into two groups $A \equiv \{1,\dots,N_A\}$ and $B \equiv \{N_A+1,\dots,N\}$, containing N_A and $N_B \equiv N - N_A$ sites, respectively. The spins living in part A and different sheets are identified, i.e., $\forall i \in A$ one has

$$S_i^{(r)} = S_i^{(r')} \quad \forall\, r, r'. \tag{11}$$

Since in each sheet all spins interact with each other, there is no notion of distance. between different spins. Thus, physical observables should depend on the booklet geometry only through the ratio $\omega \equiv N_A/N_B$.

In Eq. (10) the couplings $J_{ij} \in \mathbb{R}$ are uncorrelated quenched random variables. J_{ij} are the same in all the sheets of the booklet. Specifically, here we choose J_{ij} distributed according to the (gaussian) distribution ($P(J_{ij})$)

$$P(J_{ij}) = \left(\frac{N}{2\pi}\right)^{1/2} \exp\Big\{-\frac{N}{2}\Big(J_{ij} - \frac{J_0}{N}\Big)^2\Big\}. \tag{12}$$

The mean and the variance of $P(\{J_{ij}\})$ are given as $[J_{ij}] = J_0/N$ and $[(J_{ij} - [J_{ij}])^2] = J^2/N$, respectively. The square brackets $[\cdot]$ denote the average over different realinzations of J_{ij}. Here we restrict ourselves to $J_0 = 0$ and $J = 1$. The factors N in Eq. (12) ensure a well-defined thermodynamic limit.

The partition function $Z(\omega, n, \beta, \{J\})$ of the S-K model on the booklet at inverse temperature $\beta \equiv 1/T$, and fixed disorder realization $\{J_{ij}\}$, reads

$$Z(\omega, n, \beta, \{J\}) \equiv \mathrm{Tr}' \exp(-\beta \mathcal{H}) = \\ \mathrm{Tr}' \exp\Big\{\beta \sum_r \Big(\sum_{i<j} S_i^{(r)} S_j^{(r)} - h \sum_{i=1}^N S_i^{(r)}\Big)\Big\}, \tag{13}$$

where $\mathrm{Tr}' \equiv \sum_{\{S_i\}}$ denotes the sum over all possible spin configurations. The prime in Tr' stresses that only spin configurations satisfying the booklet constraint in Eq. (11) are considered. In the two limits $\omega \to 0$ and $\omega \to 1$ one recovers the standard S-K model. In particular, for $\omega = 0$, i.e., n disconnected sheets, from Eq. (13) one has $Z(0, n, \beta, \{J\}) = Z(\beta, \{J\})^n$, with $Z(\beta, \{J\})$ the partition function of the S-K model on the plane. On the other hand, for $\omega = 1$ it is $Z(1, n, \beta, \{J\}) = Z(n\beta, \{J\})$, i.e., the partition function of the S-K model at inverse temperature $n\beta$. The quenched averaged free energy $[F(\omega, n, \beta)]$, is defined as

$$[F(\omega, n, \beta)] \equiv -\frac{1}{\beta} \int \mathcal{D}\{J\} \log Z(\omega, n, \beta, \{J\}), \tag{14}$$

where $\int \mathcal{D}\{J\} \equiv \prod_{i<j} \int_{-\infty}^{+\infty} dJ_{ij} P(J_{ij})$. Notice that $[F(\omega, n, \beta)]$ is the main ingredient to construct the classical Rényi entropies and the mutual information (cf. Eq. (5) and Eq. (7)).

At $\omega = 0$ and $\omega = 1$ the phase diagram of the S-K model in the thermodynamic limit is well established[28]. In particular, at $\omega = 0$ the model exhibits a standard paramagnetic phase in the high temperature region, whereas at low temperatures a glassy phase is present, with replica-symmetry breaking[28]. The two phases are divided by a second order phase transition at $\beta = \beta_c = 1$. The phase diagram for $\omega = 1$ is the same, apart from the trivial redefinition $\beta \to n\beta$. We anticipate here (see section IV B) that a similar scenario holds for generic ω. Specifically, the glassy phase at low temperatures along with the replica symmetry breaking mechanism survive for generic $0 < \omega < 1$, while at high temperature the model is paramagnetic. The critical point at $\beta = \beta_c(\omega)$, which marks the transition between the two phases, is a nontrivial function of the booklet ratio ω.

B. The replicated booklet and the overlap tensor

The disorder-averaged free energy $[F(\omega, n, \beta)]$ (cf. Eq. (14)) is obtained, using the standard replica trick[41], as

$$[F(\omega, n, \beta)] = \lim_{\alpha \to 0} \frac{[Z^\alpha(\omega, n, \beta)] - 1}{\alpha}. \tag{15}$$

Here $[Z^\alpha(\omega, n, \beta)]$ is the disorder-averaged partition function of $\alpha \in \mathbb{N}$ independent copies of the S-K model on the booklet. Precisely, $[Z^\alpha(\omega, n, \beta)]$ reads

$$[Z^\alpha(\omega, n, \beta)] = \int \mathcal{D}\{J\} \mathrm{Tr}' \exp \sum_{r,\gamma} \Big\{ \\ \beta \sum_{i<j} J_{ij} S_i^{(r,\gamma)} S_j^{(r,\gamma)} + \beta h \sum_i S_i^{(r,\gamma)}\Big\}, \tag{16}$$

where the index $\gamma = 1, 2, \dots, \alpha$ labels the different fictitious replicas introduced in Eq. (15), whereas r denote the physical replicas, as in Eq. (13). Clearly, physical and fictitious replicas do not interact. Notice that $Z^\alpha(\omega, n, \beta)$ can be thought of as the partition function of the S-K model on a "replicated" booklet.

Using Eq. (12), the disorder average in Eq. (16) can be performed explicitly, to obtain

$$[Z^\alpha(\omega, n, \beta)] = \mathrm{Tr}' \exp \sum_{r,\gamma} \Big\{ \\ \frac{1}{N} \sum_{i<j} \Big(\frac{\beta^2}{2} \sum_{\gamma',r'} S_i^{(r,\gamma)} S_j^{(r,\gamma)} S_i^{(r',\gamma')} S_j^{(r',\gamma')} \\ + \beta J_0 S_i^{(r,\gamma)} S_j^{(r,\gamma)}\Big) + \beta h \sum_i S_i^{(r,\gamma)}\Big\}. \tag{17}$$

In contrast with Eq. (16), physical and unphysical replicas are now coupled by a four-spin term. It is convenient to introduce the auxiliary Hubbard-Stratonovich variables $q_{\gamma\gamma'}^{rr'}$ and m_γ^r, with $\gamma, \gamma' = 1, \dots, \alpha$ and $r = 1, \dots, n$. Following the spin glass literature[12], we dub $q_{\gamma\gamma'}^{rr'}$ the overlap tensor. In the standard S-K model (i.e., for $n = 1$) $q_{\gamma\gamma'}^{rr'}$ becomes a $\alpha \times \alpha$

matrix[20]. Eq. (17) now yields

$$[Z^\alpha(\omega,n,\beta)] = \exp\Big(\frac{\beta^2 N n\alpha}{4}\Big)\int \prod_{\substack{\gamma\le\gamma'\\ r,r'}} dq^{rr'}_{\gamma\gamma'} \int \prod_{\gamma,r} dm^r_\gamma \\ \mathrm{Tr}'\exp\Big\{ -N\mathcal{K}(\{q,m\}) + \sum_i \mathcal{L}_i(\{q,m\})\Big\}, \quad (18)$$

where we neglected subleading contributions $\mathcal{O}(1/N)$ in the thermodynamic limit. Here $\mathcal{K}(\{q,m\})$ is spin-independent and reads

$$\mathcal{K}(\{q,m\}) \equiv \frac{\beta^2}{2}\Big(\sum_{\gamma<\gamma'}\sum_{r,r'}(q^{rr'}_{\gamma\gamma'})^2 \\ + \sum_\gamma\sum_{r<r'}(q^{rr'}_{\gamma\gamma})^2\Big) + \frac{\beta}{2J_0}\sum_{\gamma r}(m^r_\gamma)^2. \quad (19)$$

On the other hand $\mathcal{L}_i(\{q,m\})$ depends on the spin degrees of freedom, and it is given as

$$\mathcal{L}_i(\{q,m\}) \equiv \beta^2 \sum_{\gamma<\gamma'}\sum_{rr'} q^{rr'}_{\gamma\gamma'} S_i^{(r,\gamma)} S_i^{(r',\gamma')} + \\ \beta^2\sum_\gamma\sum_{r<r'} q^{rr'}_{\gamma\gamma} S_i^{(r,\gamma)} S_i^{(r',\gamma)} + \beta\sum_{\gamma r}(m^r_\gamma + h) S_i^{(r,\gamma)}. \quad (20)$$

Interestingly, $\mathcal{L}_i$ describes a system of $n\alpha$ spins living in the replica space with the long-range interaction $q^{rr'}_{\gamma\gamma'}$, and a magnetic field $m^r_\gamma + h$. Notice that, while the first term in Eq. (20) is off-diagonal in the space of the fictitious replicas, the second one is diagonal. The latter fully determines the behavior of the model in the paramagnetic phase at high temperatures (see section IV A).

Since in Eq. (18) spins on different sites are decoupled, one can perform the trace over the spins in parts A and B (see Fig. 1) independently, to obtain

$$[Z^\alpha(\omega,n,\beta)] = \int \prod_{\substack{\gamma\le\gamma'\\ r,r'}} dq^{rr'}_{\gamma\gamma'} \int \prod_{\gamma,r} dm^r_\gamma \exp\Big\{N\Big(\\ \frac{\beta^2 n\alpha}{4} + \omega\log \mathrm{Tr}_A e^{\mathcal{L}} + (1-\omega)\log \mathrm{Tr}_B e^{\mathcal{L}} - \mathcal{K}\Big)\Big\}. \quad (21)$$

Here to lighten the notation we drop the dependence on the coordinate i and the arguments of $\mathcal{L}_i(\{q,m\})$ and $\mathcal{K}(\{q,m\})$. Tr_A and Tr_B denote the trace over the spin degrees of freedom living in parts A and B of the booklet. The subscript in Tr_A is to stress that spins living in different physical replicas (i.e., for $r \neq r'$ in Eq. (20)) are identified (due to the booklet constraint in Eq. (11)), whereas they have to be treated as independent variables in performing Tr_B. Notice that in Eq. (21) the trace acts over a system of $n\alpha$ spins, instead of $Nn\alpha$, as in Eq. (18).

C. The saddle point approximation

In the thermodynamic limit, i.e., for $N, N_A \to \infty$, at fixed ratio $\omega \equiv N_A/N$, one can take the saddle point approximation in Eq. (21), which yields

$$[Z^\alpha(\omega,n,\beta)] \approx \exp\Big\{N\alpha\Big(\frac{\beta^2 n}{4} - \frac{\mathcal{K}}{\alpha} \\ + \frac{\omega}{\alpha}\log \mathrm{Tr}_A \exp(\mathcal{L}) + \frac{1}{\alpha}(1-\omega)\log \mathrm{Tr}_B \exp(\mathcal{L})\Big)\Big\}. \quad (22)$$

The overlap tensor $q^{rr'}_{\gamma\gamma'}$ and m^r_γ are determined by solving the saddle point equations

$$\frac{\partial}{\partial q^{rr'}_{\gamma\gamma'}}\left(\omega\log \mathrm{Tr}_A e^{\mathcal{L}} + (1-\omega)\log \mathrm{Tr}_B e^{\mathcal{L}}\right) = q^{rr'}_{\gamma\gamma'} \quad (23)$$
$$\frac{\partial}{\partial m^r_\gamma}\left(\omega\log \mathrm{Tr}_A e^{\mathcal{L}} + (1-\omega)\log \mathrm{Tr}_B e^{\mathcal{L}}\right) = \frac{1}{J_0} m^r_\gamma.$$

It is enlightening to rewrite Eqs. (23) as

$$q^{rr'}_{\gamma\gamma'} = \omega\langle S^{(r,\gamma)} S^{(r',\gamma')}\rangle_A + (1-\omega)\langle S^{(r,\gamma)} S^{(r',\gamma')}\rangle_B \\ \frac{1}{J_0} m^r_\gamma = \omega\langle S^{(r,\gamma)}\rangle_A + (1-\omega)\langle S^{(r,\gamma)}\rangle_B \quad (24)$$

where $\langle\mathcal{O}\rangle_{A(B)} \equiv (Z_{A(B)})^{-1}\mathrm{Tr}_{A(B)}\{\mathcal{O}\exp(\mathcal{L})\}$ with $Z_{A(B)} \equiv \mathrm{Tr}_{A(B)}\exp(\mathcal{L})$. The first equation in Eqs. (24) implies that $q^{rr}_{\gamma\gamma} = 1\ \forall\gamma, r$. For $\omega = 0$ and $n = 1$, one recovers the saddle point equations for the standard SK model[12,28].

In order to calculate the free energy $[F(\omega,n,\beta)]$ one has to solve the saddle point equations (24), take the analytic continuation $\alpha \in \mathbb{R}$, and, finally, the limit $\alpha \to 0$. (cf. Eq. (15)). Although it is possible to solve the Eqs. (24) numerically for any fixed $r, \alpha \in \mathbb{N}$, taking the analytic continuation $\alpha \in \mathbb{R}$ is a formidable task, since the dependence of $Z^\alpha(\omega,n,\beta)$ on α is in general too complicated. The strategy to solve this problem is to choose a specific form of the overlap tensor $q^{rr'}_{\gamma\gamma'}$ in terms of "few" parameters, which allows to perform the analytic continuation and the limit $\alpha \to 0$ exactly.

For the standard S-K model (i.e., for $n = 1$) the simplest parametrization is the replica-symmetric one (RS), which amounts to take $q^{11}_{\gamma\gamma'} = q$. This relies on the observation that the fictitious replicas appear symmetrically in Eq. (16). Although the RS ansatz gives the correct result at high temperature, it fails in the glassy phase at low temperatures, where the permutational invariance within the replicas has to be broken[42]. A systematic scheme to break the replica symmetry, which allows to capture the the glassy behavior of the S-K model at low temperature, is the celebrated Paris ansatz[25]. We anticipate (see section V) that a similar scheme has to be used to describe the glassy phase of the S-K model on the booklet.

IV. THE REPLICA-SYMMETRIC (RS) ANSATZ

In this section we present the solution of the S-K model on the booklet, using the replica symmetric approximation. In subsection IV A we focus on the paramagnetic phase at high temperature, where this approximation is exact. In particular, we show that the behavior of the model is fully determined by the diagonal part of the overlap tensor $q^{rr'}_{\gamma\gamma'}$. The general structure of $q^{rr'}_{\gamma\gamma'}$ in the replica-symmetric (RS) ansatz is discussed

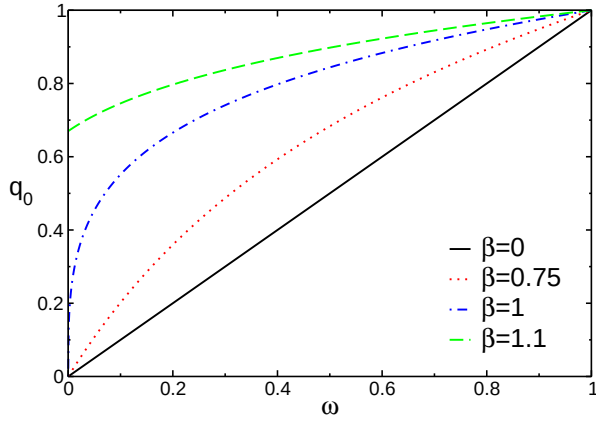

FIG. 2. The S-K model on the 2-sheets booklet with zero magnetic field in the paramagnetic phase: the solution q_0 of the saddle point equation Eq. (32) plotted as a function of the ratio ω and for $\beta = 1/T = 0, 3/4, 1, 4/3$. At $\omega = 1$ one has $q_0 = 1, \forall\beta$. In the zero-temperature limit $\beta \to \infty$ it is $q_0 \to 1, \forall\omega$. The straight line is the infinite temperature result.

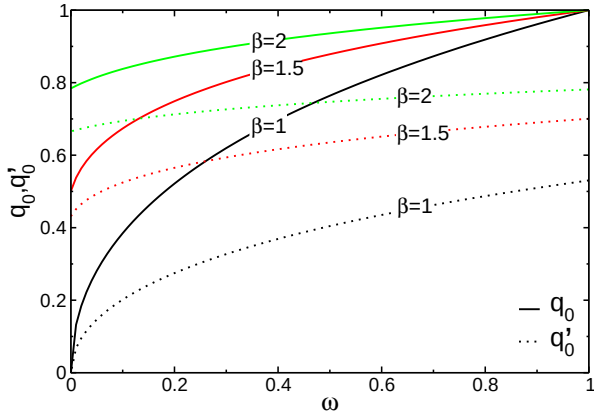

FIG. 3. The S-K model on the 2-sheets booklet with zero magnetic field. The overlap tensor in the replica-symmetric (RS) approximation (see Eq. (33)): the solutions q_0 and q_0' (shown as full and dotted lines, respectively) of the saddle point equations Eqs. (A1)(A2) plotted as a function of the ratio ω, and inverse temperature $\beta = 1/T = 1, 3/2, 2$. At $\omega = 1$ one has that $q_0 = 1, \forall\beta$. In the limit $\beta \to \infty$ it is $q_0, q_0' \to 1, \forall\omega$.

in subsection IV B. This allows to determine the critical temperature of the paramagnetic-glassy transition. Similar to the standard S-K model, the RS ansatz is not correct in the low-temperature region.

A. The paramagnetic phase

Here we provide the exact analytical expression for the free energy $[F_{para}(\omega, n, \beta)]$ in the paramagnetic non-glassy phase of the S-K model on the booklet. We start discussing the infinite temperature limit (i.e., $\beta \to 0$).

Using Eq. (20) one obtains $\mathrm{Tr}_A e^{\mathcal{L}} = 2^\alpha + \mathcal{O}(\beta^2)$ and $\mathrm{Tr}_B e^{\mathcal{L}} = 2^{n\alpha} + \mathcal{O}(\beta^2)$, implying

$$\langle S^{(r,\gamma)} S^{(r',\gamma')} \rangle_B = 2^{n\alpha} \delta_{\gamma,\gamma'} \delta_{r,r'} + \mathcal{O}(\beta^2) \qquad (25)$$
$$\langle S^{(r,\gamma)} S^{(r',\gamma')} \rangle_A = 2^{\alpha} \delta_{\gamma,\gamma'} + \mathcal{O}(\beta^2).$$

After substituting in Eqs. (24), it is straightforward to obtain the infinite-temperature overlap tensor $q^{rr'}_{\gamma\gamma'}$ as

$$q^{rr'}_{\gamma\gamma'} = (1-\omega)\delta_{\gamma,\gamma'}\delta_{r,r'} + \omega\delta_{\gamma,\gamma'}. \qquad (26)$$

Remarkably, $q^{rr'}_{\gamma\gamma'}$ becomes diagonal in both the indices γ, γ' and r, r', i.e., the physical and fictitious replica spaces. The analytic continuation $\alpha \to 0$ (cf. Eq. (15)) can be performed explicitly, to obtain

$$[F_{para}(\omega, n, \beta)] = N\Big\{ (n - \omega(n-1)) \log(2) + \frac{\beta^2}{4}(\omega^2(n^2-n) + n) \Big\} + \mathcal{O}(\beta^4). \qquad (27)$$

It is natural to expect that for arbitrary $\beta \leq \beta_c$, with β_c the critical temperature of the paramagnetic-glassy transition, the overlap tensor $q^{rr'}_{\gamma\gamma'}$ remains diagonal. This suggests the ansatz

$$q^{rr'}_{\gamma\gamma'} = (1-q_0)\delta_{r,r'}\delta_{\gamma,\gamma'} + q_0\delta_{\gamma,\gamma'}. \qquad (28)$$

with $q_0 \in \mathbb{R}$ a parameter. The ansatz (28) is formally obtained from Eq. (26) by replacing $\omega \to q_0$. Notice that one has $q^{rr}_{\gamma\gamma} = 1$, in agreement with Eqs. (24). Using Eq. (28), one obtains $\mathcal{L}_{para}$ (cf. Eq. (20)) as

$$\mathcal{L}_{para} = \beta^2 \frac{q_0}{2} \Big\{ \sum_\gamma \sum_{rr'} S^{(r,\gamma)} S^{(r',\gamma)} - n\alpha \Big\}. \qquad (29)$$

After introducing the auxiliary Hubbard-Stratonovich variables z_λ (with $\lambda = 1, \ldots, \alpha$), one can write

$$\mathrm{Tr}_B \exp(\mathcal{L}_{para}) = \mathrm{Tr}_B \int \prod_\lambda Dz_\lambda \exp\Big(z_\lambda \beta \sqrt{q_0} \sum_r S^{(r,\lambda)} \Big), \qquad (30)$$

where $\int Dz f(z) \equiv (2\pi)^{-1/2} \int \exp(-z^2/2) f(z)$. Notice that due to the square root in Eq. (30), one has the constraint $q_0 > 0$. Moreover, from Eq. (29) one obtains $\mathrm{Tr}_A \exp(\mathcal{L}) = 2^{n\alpha}$. The trace Tr_B in Eq. (30) can be performed explicitly. Using Eq. (22) and Eq. (15), one obtains the free energy $[F_{para}(\omega, n, \beta)]$ as

$$[F_{para}(\omega, n, \beta)] = N\Big\{ n\log(2) - \omega(n-1)\log(2) + \beta^2 \Big(\frac{n}{4} - \frac{q_0^2}{4}(n^2-n) + \frac{\omega}{2} q_0 n^2 - q_0 n \Big) + (1-\omega) \log \int Dz \cosh^n(z\sqrt{q_0}\beta) \Big\}, \qquad (31)$$

where q_0 is determined by solving the saddle point condition $\partial[F_{para}(\omega, n, \beta)]/\partial q_0 = 0$. For the 2-sheets booklet (i.e., $n = 2$) this is given as

$$q_0 = \omega + (1-\omega)\tanh(\beta^2 q_0). \qquad (32)$$

Alternatively, Eq. (32) can be obtained by substituting the ansatz (28) in Eqs. (24).

Clearly, for two independent copies of the S-K model (i.e., $\omega = 0$) Eq. (32) gives $q_0 = 0$ for $\beta \leq 1$, whereas one obtains $q_0 \neq 0$ for $\beta > 1$. On the other hand, for $\omega = 1$ one has $q_0 = 1\ \forall \beta$. For generic $0 < \omega < 1$ the solution of Eq. (32) is shown in Figure 2, plotting q_0 as a function of ω, for $\beta = 0, 0.75, 1, 1.1$. For $\beta = 0$ it is $q_0 = \omega$ (straight line in the Figure). In the low-temperature limit one has $q_0 \to 1$, for any ω. In particular, it is straightforward to check that $q_0 \approx 1 - 2(1-\omega)\exp(-2\beta^2)$ for $\beta \to \infty$.

B. The replica-symmetric (RS) approximation

In the replica-symmetric (RS) approximation one writes the overlap tensor $q^{rr'}_{\gamma\gamma'}$ as

$$q^{rr'}_{\gamma\gamma'} = (1-q_0)\delta_{r,r'}\delta_{\gamma,\gamma'} + q_0\delta_{\gamma,\gamma'} + (1-\delta_{\gamma,\gamma'})q'_0. \quad (33)$$

The first two terms in Eq. (33) are the same as in the paramagnetic phase (cf. Eq. (28)). The last term sets $q^{rr'}_{\gamma\gamma'} = q'_0$ $\forall \gamma \neq \gamma'$ and $\forall r, r'$. Physically, Eq. (33) means that we require the permutational symmetry in both the physical and fictitious replica space. We do not have any rigorous argument to justify the ansatz (33), besides its simplicity. However, we numerically observe that it captures quite accurately the behavior of the model, at least around the paramagnetic-glassy transition (see section VI for the Monte Carlo results).

Using Eq. (33) and Eqs. (15)(22) one obtains the replica-symmetric approximation for the free energy $[F_{RS}(\omega, n, \beta)]$ as

$$[F_{RS}(\omega,n,\beta)] = \lim_{\alpha\to 0}\Big\{N\Big[\frac{\beta^2}{4}n - \frac{\beta^2}{4}\Big((q_0^2 - (q'_0)^2)n^2 - q_0^2 n\Big) + \frac{1-\omega}{\alpha}\log \mathrm{Tr}_B \exp(\mathcal{L}_{RS}) + \frac{\omega}{\alpha}\log \mathrm{Tr}_A \exp(\mathcal{L}_{RS})\Big]\Big\}, \quad (34)$$

where $\mathcal{L}_{RS}$ is obtained by substituting Eq. (33) in Eq. (20), which yields

$$\mathcal{L}_{RS} = \frac{q'_0}{2}\beta^2 \sum_{\gamma\gamma'}\sum_{rr'} S^{(r,\gamma)}S^{(r',\gamma')} + \frac{q_0 - q'_0}{2}\beta^2 \sum_{\gamma}\sum_{rr'} S^{(r,\gamma)}S^{(r',\gamma')} - \frac{q_0}{2}\beta^2 n\alpha. \quad (35)$$

To calculate the last two terms in Eq. (34) one has to introduce two auxiliary Hubbard-Stratonovich variables z, z', similar to the paramagnetic phase (cf. section IV A). Thus, after performing the trace over the spin variables, in the limit $\alpha \to 0$, one obtains

$$\log \mathrm{Tr}_B \exp(\mathcal{L}_{RS}) = -\frac{q_0}{2}\beta^2 n\alpha + n\alpha\log(2) + \alpha\int Dz \log\int Dz' H^n_{RS}(z,z'), \quad (36)$$

$$\log \mathrm{Tr}_A \exp(\mathcal{L}_{RS}) = -\frac{q_0}{2}\beta^2 n\alpha + \alpha\log(2) + \alpha\int Dz \log\int Dz' H_{RS}(nz,nz'), \quad (37)$$

where we define $H_{RS}(z,z') \equiv \cosh(\beta z\sqrt{q'_0} + \beta z'\sqrt{q_0 - q'_0})$. Notice that because of the square roots in the definition of $H_{RS}(z,z')$, one has the constraint $0 \leq q'_0 \leq q_0 \leq 1$.

In Eq. (36)(37) q_0, q'_0 have to satisfy the saddle point conditions $\partial[F_{RS}(\omega,n,\beta)]/\partial q_0 = \partial[F_{RS}(\omega,n,\beta)]/\partial q'_0 = 0$ (cf. Eqs. (A1)(A2) for the precise form of the saddle point equations for $n = 2$). The resulting q_0 and q'_0 are plotted in Figure 3 (full and dotted lines, respectively) as function of ω and for several values of β. Clearly, for any β one has $q_0 = 1$ in the limit $\omega \to 1$. Also, in the zero-temperature limit $\beta \to \infty$ one has that $q_0 \to 1$ and $q'_0 \to 1$, for any ω. Moreover, a simple calculation yields

$$q_0 = 1 - (1-\omega)\sqrt{\frac{2}{\pi}}\frac{1}{\beta}\exp\Big(-\frac{1}{\pi} - \sqrt{\frac{2}{\pi}}\beta\Big) + \dots \quad (38)$$
$$q'_0 = 1 - \frac{1}{\sqrt{2\pi}\beta} - \frac{1}{2\pi\beta^2} + \mathcal{O}(\beta^{-3}),$$

with the dots denoting exponentially suppressed terms. Interestingly, from Eq. (38) one has that $q_0 \to 1$ exponentially in the limit $\beta \to \infty$, as in the paramagnetic phase (cf. section IV A), whereas $q'_0 - 1 \propto 1/\beta$, similar to the standard SK model[28].

Finally, using the replica-symmetric ansatz Eq. (33) one can determine the critical temperature β_c of the paramagnetic-glassy transition. Near the glassy transition one should expect $q'_0 \to 0$, whereas q_0 should remain finite ($q_0 > 0$

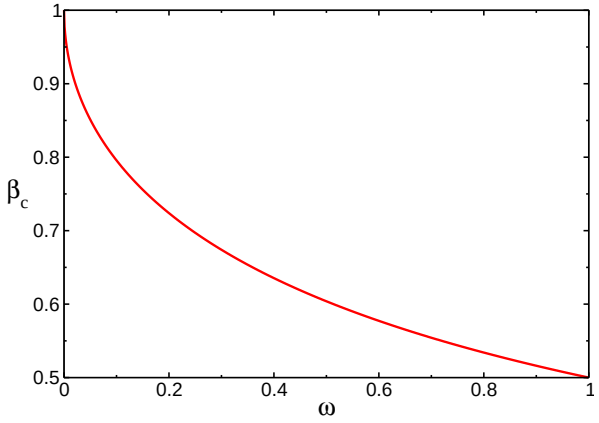

FIG. 4. The critical temperature $\beta_c \equiv 1/T_c$ for the S-K model on the 2-sheets booklet (see Fig. 1) with zero magnetic field: β_c as a function of the booklet ratio $\omega \equiv N_A/N$. Here β_c is obtained from the replica-symmetric (RS) approximation of the model. Notice that one has $\beta_c = 1$ and $\beta_c = 1/2$ for $\omega = 0$ and $\omega = 1$, respectively.

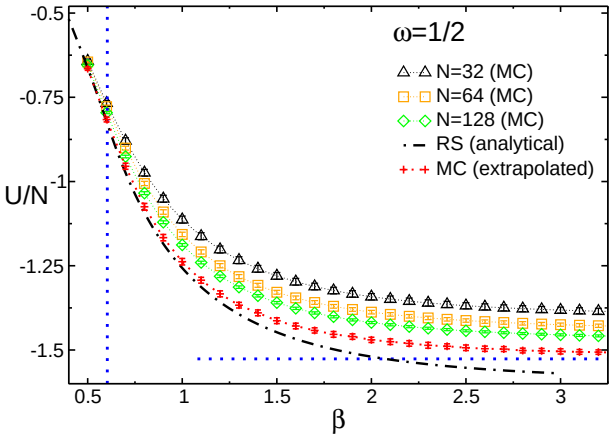

FIG. 5. The S-K model on the 2-sheets booklet with zero magnetic field and booklet ratio $\omega = 1/2$ (see Fig. 1): The internal energy per spin U/N as a function of the inverse temperature β. The triangles, squares, and rhombi, denote the Monte Carlo data for a booklet with $N = 32, 64, 128$ spins per sheet. The plus symbols are the extrapolations to the thermodynamic limit $N \to \infty$, at fixed ω. The dash-dotted line is the analytical result U_{RS}/N obtained using the replica-symmetric (RS) approximation. The horizontal dotted line is the exact zero-temperature result $U/N \approx -1.52642$.

in the paramagnetic phase, see section IV A). By expanding $[F_{RS}(\omega, n, \beta)]$ (cf. Eq (34)) for small q_0', and keeping only terms up to $\mathcal{O}((q_0')^2$, one obtains a standard Landau theory. Thus, β_c is obtained imposing that the coefficient of the quadratic term $q_0'^2$ changes sign. This leads to the equation

$$\exp(-4q_0\beta_c^2) + 2\exp(-2q_0\beta_c^2) = \frac{1-4\beta_c^2}{4\beta_c^2\omega - 1}, \qquad (39)$$

where q_0 is obtained by solving the high-temperature saddle point equation (32). The resulting β_c solution of Eq. (39) is shown in Fig. 4 as a function of ω.

V. THE ONE-STEP REPLICA-SYMMETRY-BROKEN (1-RSB) APPROXIMATION

In this section we go beyond the replicas-ymmetric approximation, including some of the effects of the replica symmetry breaking. More specifically, here we discuss the one-step replica symmetry breaking (1-RSB) approximation for the S-K model on the booklet. The overlap tensor $q^{rr'}_{\gamma\gamma'}$ now reads

$$q^{rr'}_{\gamma\gamma'} = (1-q_0)\delta_{\gamma,\gamma'}\delta_{r,r'} + q_0\delta_{\gamma,\gamma'} + (1-\delta_{\gamma,\gamma'})q', \qquad (40)$$

which is formally equivalent to the RS ansatz in Eq. (33), apart from the trivial redefinition $q_0' \to q'$. However, in contrast with Eq. (33), where $q_0' \in \mathbb{R}$ is a number, here q' is a matrix. Inspired by the Parisi scheme for the standard S-K model[25], we choose

$$q' = \begin{cases} q_1' & \text{if } \lfloor \gamma/m_1 \rfloor = \lfloor \gamma'/m_1 \rfloor \\ \\ q_0' & \text{otherwise} \end{cases}$$

where now $q_0', q_1' \in \mathbb{R}$, $m_1 \in \mathbb{N}$, and $\lfloor \cdot \rfloor$ denotes the floor function. The off-diagonal elements of q' do not depend on r, r', meaning that, although the permutational symmetry between the fictitious replicas is broken, the symmetry among the physical ones is preserved. Notice that the choice in Eq. (V) corresponds to a simple block diagonal structure for q': the elements in the $m_1 \times m_1$ diagonal blocks are set to q_1', whereas all the off-diagonal elements are set to q_0'. As for the replica-symmetric ansatz in Eq. (33), we do not have any rigorous argument to justify Eq. (V) (see section (VI), for numerical results).

The effective interaction $\mathcal{L}_{1\text{-}RSB}$ (cf. Eq. (20)) in the replica space is obtained by substituting Eq. (40) in Eq. (20). This yields

$$\mathcal{L}_{1\text{-}RSB}/\beta^2 = -\frac{q_0}{2}n\alpha - \frac{q_1'-q_0}{2}\sum_{\sigma=1}^{\alpha/m_1}\sum_{\gamma\in B_\sigma}\Big(\sum_r S^{(r,\gamma)}\Big)^2 + \frac{q_0'}{2}\Big(\sum_{\gamma,r} S^{(r,\gamma)}\Big)^2 - \frac{q_0'-q_1'}{2}\sum_{\sigma=1}^{\alpha/m_1}\Big(\sum_{\gamma\in B_\sigma,r} S^{(r,\gamma)}\Big)^2, \qquad (41)$$

where we defined $B_\sigma \equiv [\sigma m_1, (\sigma+1)m_1)$ with $\sigma \in \mathbb{N}$. It is convenient t to introduce the Hubbard-Stratonovich variables $z, z_\sigma, z_{\sigma,\gamma}$ (one for each term in Eq. (41)). One then obtains

$$\log \mathrm{Tr}' \exp(\mathcal{L}_{1\text{-}RSB}) = -\frac{q_0}{2}\beta^2 n\alpha + \log \mathrm{Tr}' \int Dz \prod_\sigma \int Dz_\sigma \prod_{\gamma\in B_\sigma} \int Dz_{\sigma,\gamma} \prod_r \exp\Big\{\beta\Big[z\sqrt{q_0'}S^{(r,\gamma)} + z_{\sigma,\gamma}\sqrt{q_0-q_1'}S^{(r,\gamma)} + z_\sigma\sqrt{q_1'-q_0'}S^{(r,\gamma)}\Big]\Big\}$$

The trace over the spin variables can now be performed explicitly. Finally, one obtains the 1-RSB approximation for the free energy $[F_{1\text{-}RSB}(\omega, n, \beta)]$ as

$$[F_{1\text{-}RSB}(\omega, n\beta)]/N = (\omega + (1-\omega)n)\log(2) + \frac{n}{4}\beta^2\Big(1 + nq_0'^2 - n(m_1-1)(q_1'^2 - q_0'^2) - (n-1)q_0^2 - 2q_0\Big) + \int Dz\Big\{\frac{\omega}{m_1}\log\int Dz'\Big\{\int Dz'' H^n_{1\text{-}RSB}(z,z',z'')\Big\}^{m_1} + \frac{1-\omega}{m_1}\log\int Dz'\Big\{\int Dz'' H_{1\text{-}RSB}(nz, nz', nz'')\Big\}^{m_1}\Big\}, \qquad (42)$$

where we defined $H_{1\text{-}RSB}(z,z',z'')$ as

$$H_{1\text{-}RSB}(z,z',z'') \equiv \cosh(z\beta\sqrt{q_0'} + z''\beta\sqrt{q_0-q_1'} + z'\beta\sqrt{q_1'-q_0'}) \quad (43)$$

Similar to the replica-symmetric situation (see section IV B), from Eq. (43) one has the constraint $0 \le q_0' \le q_1' \le q_0 \le 1$. The parameters q_0, q_0', q_1', m_1 are obtained by solving the saddle point equations Eqs. (A7)(A8)(A9) (A10). One should remark that, although $m_1 \in \mathbb{N}$ in Eq. (V), one obtains $m_1 \in \mathbb{R}$ from the saddle point equations. Finally, the RS result $F_{RS}(\omega,n,\beta)$ is recovered from Eq. (42) in the limit $q_1' \to q_0'$, while the paramagnetic solution corresponds to $q_1' \to q_0' \to 0$.

VI. MONTE CARLO RESULTS: THE INTERNAL ENERGY

In this section we numerically confirm the results of section IV. To this purpose, we discuss Monte Carlo (MC) data for the S-K model on the 2-sheets booklet with zero external magnetic field. We focus on the internal energy $U(\omega,n,\beta)$

$$U(\omega,n,\beta) \equiv -\frac{\partial}{\partial\beta}[\log(Z(\omega,n,\beta))]. \quad (44)$$

Fig. 5 plots the MC data for $U(\omega,2,\beta)$ versus the inverse temperature β, for the booklet with $\omega = 1/2$ (see Fig. 1). The cicles, squares, and triangles are the MC results for different sizes (i.e., number of spins per sheet) $N = 32, 64, 128$. The vertical dotted line is the critical temperature $\beta_c \approx 0.603$ of the paramagnetic-glassy transition (cf. Fig. 4). Clearly, in the high-temperature region for $\beta < \beta_c$ finite size effects are small, and already for $N = 64$ the MC data are indistinguishable from the result in the thermodynamic limit. Oppositely, stronger scaling corrections are visible in the low-temperature phase at $\beta > \beta_c$. The plus symbols in Fig. 5 are the numerical extrapolations in the thermodynamic limit $N \to \infty$. These are obtained by fitting the finite size MC data to the ansatz $U(\omega,\beta)/N = u_\infty(\omega,\beta) + c/N^\phi$, where u_∞ is energy density in the thermodynamic limit, c a fitting parameter, and ϕ the exponent of the scaling corrections. In our fits we fix $\phi = 2/3$, which is the exponent governing the finite-size corrections of U/N in the standard S-K model[37,38].

The dash-dotted line is the analytical result U_{RS} obtained using the replica-symmetric (RS) approximation (see section IV B). Using Eq (44) and Eq. (34), U_{RS} is obtained as

$$U_{RS} = -N\beta(1 + q_0^2 - 2q_0'^2). \quad (45)$$

Here q_0, q_0' are solutions of the saddle point equations Eqs. (A1) (A2). Notice that U_{RS} depends on ω only through q_0, q_0'. From Fig. 5 one has that, while U_{RS} is in perfec agreeement with the numerics for $\beta \approx \beta_c$, deviations appear in the low-temperature region. Moreover, these deviations increase upon lowering the temperature, and already at $\beta \gtrsim 1$, U_{RS} is incompatible with the data. This is has to be attributed to the replica symmetry breaking happening in the glassy phase.

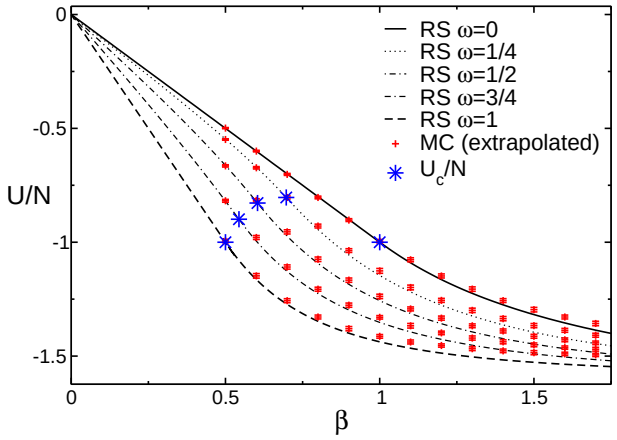

FIG. 6. The S-K model on the 2-sheets booklet and zero magnetic field: The internal energy per spin U/N in the thermodynamic limit. The symbols are the Monte Carlo data extrapolated to the thermodynamic limit $N \to \infty$, at fixed booklet ratio ω (see Fig. 1). U/N is plotted as a function of inverse temperature β and for $\omega = 0, 1/4, 1/2, 3/4, 1$. The lines are the analytical results U_{RS} obtained using the replica-symmetric (RS) approximation. The stars denote the value of U_c/N at the paramagnetic-glassy transition.

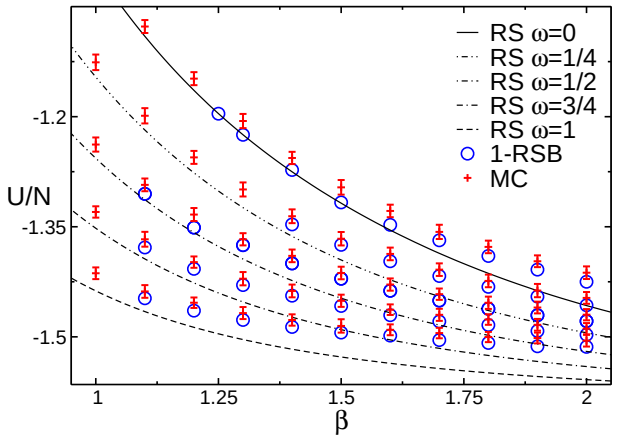

FIG. 7. The S-K model on the 2-sheets booklet with zero magnetic field: The internal energy per spin U/N in the thermodynamic limit plotted as a function of inverse temperature β. The plus symbols are the same Monte Carlo data as in Figure 6. The lines denote U/N in the replica-symmetric (RS) approximation (same as in Fig. 6). The circles are the results in the one-step replica symmetry breaking (1-RSB) approximation.

Finally, since in the limit $\beta \to \infty$ all the physical replicas are in the same state, one should expect that $u_\infty(\omega,\beta) \to n u_\infty(0,\beta)$ (horizonthal line in Fig. 5), with $u_\infty(0,\beta) \to -0.76321...$[25,26] the zero-temperature internal energy density of the S-K model on a single sheet. Surprisingly, this behavior is already observed in the MC data at $\beta \approx 3$, whereas it is not captured correctly by the RS approximation.

The behavior of U/N for $\omega \neq 1/2$ is investigated in Fig. 6, plotting U/N as a function of β for $\omega = 0, 1/4, 1/2, 3/4, 1$. The plus symbols are the MC data extrapolated in the thermodynamic, at fixed ω. Similar to Fig. 6, the extrapolations are

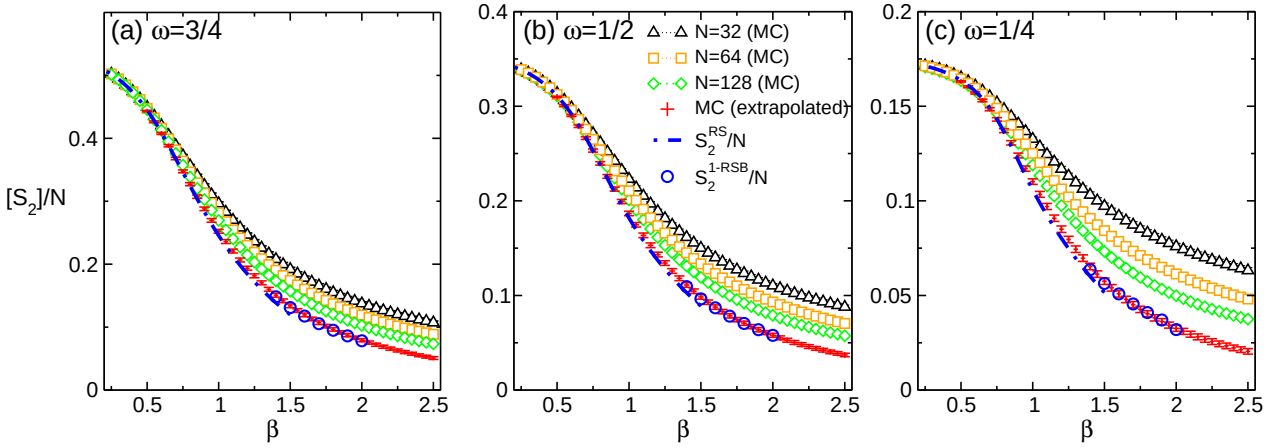

FIG. 8. The classical Renyi entropy per spin $S_2(\omega)/N$ in the S-K model on the 2-sheets booklet with zero magnetic: $S_2(\omega)/N$ as a function of the inverse temperature β. The different panels correspond to different booklet ratios $\omega = 3/4, 1/2, 1/4$ (see Fig. 1). The triangles, squares and rhombi denote the Monte Carlo results for booklets with $N = 32, 64, 128$ spins per sheet. The plus symbols are the numerical extrapolations to the thermodynamic limit. The dash-dotted lines are the analytical results U_{RS}/N using the replica-symmetry (RS) approximation. The circles are the analytical results $U_{1\text{-}RSB}$ obtained using the one-step replica symmetry breaking (1-RSB) ansatz.

done assuming $U/N(\omega, n, \beta) = u_\infty(\omega, n, \beta) + c/N^\phi$, with $\phi = 2/3$ irrespective of ω. The stars in Fig. 6 are the critical values U_c/N at the paramagnetic-glassy transition. Specifically, here β_c is obtained by numerically solving Eq. (39). The lines in Fig. 6 denote the replica-symmetric result U_{RS} (cf. Eq. (45)).

For generic n and ω, in the limit $\beta \to 0$, Eq. (44) and Eq. (27) give

$$U_{RS}(\omega, n, \beta) = -N\frac{\beta}{2}(\omega^2(n^2 - n) + n) + \mathcal{O}(\beta^2), \quad (46)$$

i.e., a linear behavior of U/N as a function of β. For $\omega = 0$ and $\omega = 1$ this behavior is exact up to the critical point at $\beta = \beta_c$, meaning that the higher orders $\mathcal{O}(\beta^2)$ in Eq. (46) are zero. This is only an approximation at intermediate $0 < \omega < 1$. Clearly, Fig. 6 confirms that at $\beta < \beta_c$ both Eq. (45) and Eq. (46) are in excellent agreement with the numerical results. However, one should observe that U_{RS} is not correct in the low-temperature at $\beta > \beta_c$, where the replica symmetry breaking has to be taken into account.

The effects of the replica symmetry breaking are more carefully discussed in Fig. 7, plotting U/N versus $1 \le \beta \le 2$. The plus symbols and the lines are the same as in Fig. 6. The full circles denote the internal energy per spin $U_{1\text{-}RSB}/N$ as obtained using the 1-step replica symmetry breaking (1-RSB) approximation (see section V). Specifically, from Eq. (42) and Eq. (44), for $n = 2$ a straightforward calculation gives

$$U_{1\text{-}RSB} = -N\beta(1 + q_0^2 + 2q_1'^2(m_1 - 1) - 2q_0'^2 m_1), \quad (47)$$

where $q_0, q_0', q_1', m_1 \in \mathbb{R}$ are solutions of the saddle point equations (A7)-(A10). Clearly, from Eq. (47) one has $U_{1\text{-}RSB} \to U_{RS}$ for $q_1' \to q_0'$, as expected. Moreover, since for $\beta \approx \beta_c$ it is $q_1' \approx q_0' \approx 0$, one has that $U_{RSB} \approx U_{RS}$, i.e. the effects of the replica symmetry breaking are negligible near the critical point. On the other hand, in the replica symmetry broken phase at low temperature, where the RS approximation U_{RS} fails (see Fig. 6), $U_{1\text{-}RSB}$ is in good agreement with the Monte Carlo data, at least up to $\beta \approx 2$. This allows us to conclude that, although the ansatz in Eq. (40) might not be correct in the limit $\beta \to \infty$, it captures some of the effects of the replica symmetry breaking.

VII. THE CLASSICAL RÉNYI ENTROPIES

We now turn to discuss the behavior of the classical Rényi entropies (cf. Eq. (7)) in the S-K model. Here we restrict ourselves to the second Rényi entropy S_2. Due to the mean-field nature of the S-K model (cf. Eq. (10)), there is no boundary between the two parts A and B of the system (see Fig. 1), implying that S_2 exhibits the volume law $S_2 \propto N$, rather than the area law. Therefore it is natural to consider the entropy per spin S_2/N.

The Monte Carlo data for S_2/N are shown in Fig. 8 plotted versus the inverse temperature $0.25 \le \beta \le 2.5$. The different panels correspond to the booklet ratios $\omega = 3/4, 1/2, 1/4$ (see Fig. 1). In all panels the empty circles, squares, and rhombi correspond to booklets with $N = 32, 64, 128$ spins per per sheet. Clearly, finite size effects are present, which increase upon lowering the temperature, as expected. In order to obtain S_2/N in the thermodynamic limit we fit the data to the ansatz $S_2(\omega) = s_2(\omega) + c'(\omega)/N^{\phi'}$, where $s_2(\omega)$ is the entropy per spin in the limit $N \to \infty$, c' a constant, and ϕ' the exponent of the scaling corrections. The plus symbols in Fig. 8 are the results of the fits. We should mention that the fits give $\phi' \approx 2/3$, which is the exponent of the scaling corrections of the free energy in the standard S-K model. This is not surprising, since $S_2(\omega)$ is obtained as the difference $S_2(\omega) \equiv [F(0, 2, \beta) - F(\omega, 2, \beta)]$ (cf. Eq. (7)). Clearly, in the thermodynamic limit $S_2(\omega)/N$ is finite for any β, confirming the expected volume law $S_2 \propto N$ behavior. Moreover, S_2/N exhibits a maximum in the infinite-temperature limit $\beta \to 0$. The height of this maximum is a decreasing function of ω

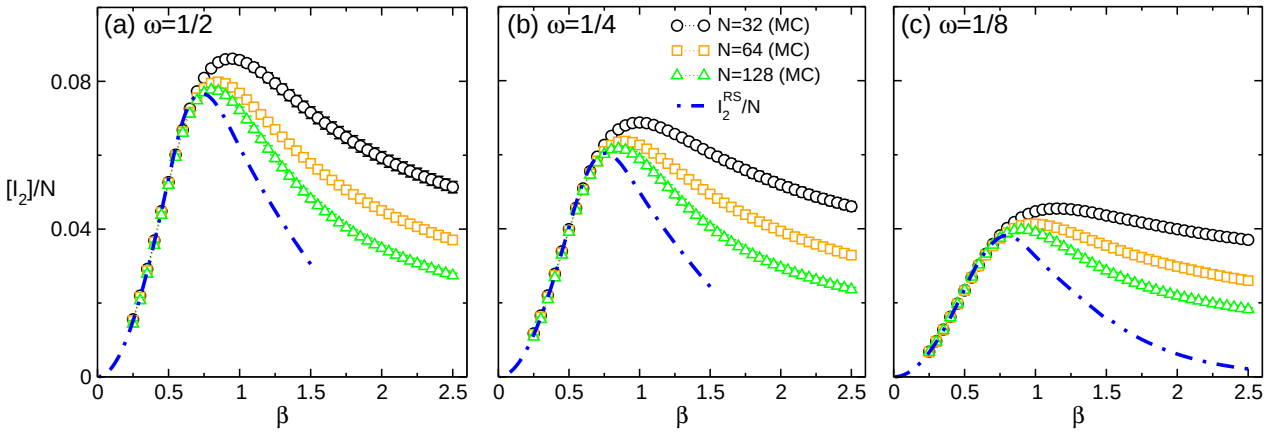

FIG. 9. The classical mutual information per spin $\mathcal{I}_2/N$ in the S-K model on the 2-sheets booklet with zero magnetic field: $\mathcal{I}_2/N$ versus the inverse temperature β. The different panels correspond to different booklet ratios $\omega = 1/2, 1/4, 1/8$ (see Fig. 1). The same scale is used on both axes in all panels. The symbols are the Monte Carlo data for systems with $N = 32, 64, 128$ spins per sheet. The dash-dotted line is the analytical result in the replica-symmetric (RS) approximation.

(compare the panels (a)(b)(c) in Fig. 8). Finally, for any fixed ω, $S_2(\omega)$ decreases smoothly upon lowering the temperature. In particular, the Monte Carlo data suggest a vanishing behavior in the zero-temperature limit $\beta \to \infty$.

The dash-dotted line in Fig. 8 denotes the analytical result S_2^{RS} obtained using the replica-symmetric (RS) approximation (see section IV B). More precisely, S_2^{RS}/N is obtained from Eq. (7) and the expression for the replica symmetric free energy $[F_{RS}]$ (cf. Eq. (34)). Notice that in the high-temperature limit $\beta \to 0$, where the RS approximation is exact, Eq. (7) and Eq. (31) give

$$S_2^{RS}(\omega) = \omega \log(2) - \frac{\beta^2}{4}\omega^2 + \mathcal{O}(\beta^2). \tag{48}$$

From Fig 8 one has that the extrapolated MC data are in quantitative agreement with S_2^{RS}/N for $\beta \lesssim 1.5$, whereas strong deviations are observed at lower temperatures (not shown in the Figure). These are reflecting the symmetry breaking. A better approximation for $S_2(\omega)/N$ at low temperatures is obtained by including the effects of the replica symmetry breaking. The full circles in Fig. 8 are the analytical results $S_2^{1\text{-}RSB}$ obtained using the one step replica symmetry breaking (1-RSB) ansatz (see section V). $S_2^{1\text{-}RSB}$ is formally obtained using Eq. (7) and the free energy $[F_{1\text{-}RSB}]$ (cf. Eq. (42)). Remarkably, $S_2^{1\text{-}RSB}$ is in excellent agreement with the Monte Carlo extrapolations for $\beta \lesssim 2$, where the RS approximation fails.

VIII. THE CLASSICAL RÉNYI MUTUAL INFORMATION

Here we focus on the behavior of the Renyi mutual information $\mathcal{I}_2$ in the S-K model. Similar to $S_2(\omega)$, the mutual information obeys the volume law $\mathcal{I}_2(\omega) \propto N$. This is in contrast with local models, where $\mathcal{I}_n(\omega)$ exhibits an area law. Here we consider the mutual information per spin $\mathcal{I}_2(\omega)/N$.

Figure 9 $\mathcal{I}_2/N$ versus $0 \le \beta \le 2.5$ and $\omega = 1/2, 1/4, 1/8$ (panels from left to right in the Figure). Notice that by definition (cf. Eq. (5)) $\mathcal{I}_n(\omega) = \mathcal{I}_n(1-\omega)$. Circles, squares, and rhombi in Fig. 9 are Monte Carlo data for $N = 32, 64, 128$. In the high-temperature region $\mathcal{I}_2$ exhibits a clear vanishing behavior, for any $0 < \omega < 1$. Moreover, finite size effects are "small". Using Eq. (27) it is straightforward to derive the high-temperature behavior of $\mathcal{I}_n(\omega)$ as

$$\mathcal{I}_n(\omega) = \frac{N\beta^2}{2}\omega(1-\omega)n + \mathcal{O}(\beta^4). \tag{49}$$

At lower temperatures $\mathcal{I}_2/N$ increases monotonically up to $\beta \approx 1$, where it exhibits a maximum. Interestingly, the largest value of $\mathcal{I}_2/N$ ($\mathcal{I}_2/N \approx 0.09$ for $\omega = 1/2$) is quite small, as it is observed in local spin models[30]. The height of the maximum decreases as a function of ω. Its position is not simply related to the paramagnetic-glassy transition at $\beta = 1$ of the standard S-K model. This is not surprising because $\mathcal{I}_n(\omega)$ is constructed by combining the partition functions of the S-K model on the booklets with ratios ω, $1-\omega$, $\omega = 0$, and $\omega = 1$ (cf. Eq. (5)), and the critical temperature of the paramagnetic-glassy transition is a non trivial function of ω (see Fig. 4). As a consequence, the geometric mutual information $\mathcal{G}_n$ (cf. (9)) is not well defined for the S-K model. Furthermore, the curves for $\mathcal{I}_2/N$ calculated at different sizes do not exhibit any crossing at $\beta = 1$, in sharp contrast with local models[30], for which it has been shown that $\mathcal{I}_n(\omega)/N$ exhibits a crossing at a second order phase transition. For $\beta \gtrsim 1$, $\mathcal{I}_2$ decreases monotonically, for any N. The dash-dotted line in Fig. 9 denotes the analytical result obtained using the replica symmetric (RS) approximation (see section IV B). Formally this is obtained using Eq (5) and Eq. (34). This is in perfect agreement with the MC data in the whole paramagnetic phase.

Interestingly, at low temperatures $\mathcal{I}_2/N$ exhibits strong finite-size corrections, and significant deviations from the RS result. In order to extract the thermodynamic behavior of $\mathcal{I}_2/N$ we fit the MC data to

$$\frac{\mathcal{I}_2}{N} = a + \frac{b}{N^\gamma} \tag{50}$$

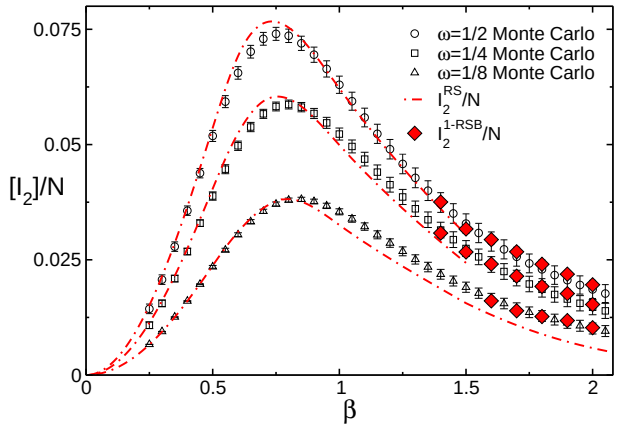

FIG. 10. The classical mutual information per spin $\mathcal{I}_2/N$ in the SK model on the 2-sheets booklet with zero magnetic field: $\mathcal{I}_2$ plotted versus β. The symbols denote the Monte Carlo results extrapolated to the thermodynamic limit for booklet ratios $\omega = 1/2, 1/4, 1/8$ (circles, squares, triangles). The dash-dotted lines are the analytical results in the replica-symmetric (RS) appproximation. The full symbols (rhombi) are the results in the first-step replica-symmetry-breaking (1-RSB) approximation.

where we fix $\gamma = 2/3$. The results of the fits are shown in Fig. 10. The circles, squares, and triangles denote $\mathcal{I}_2/N$ in the thermodynamic limit $N \to \infty$ for $\omega = 1/2, 1/4, 1/8$. Interestingly, we numerically checked that in the zero-temperature limit the data support the vanishing behavior as $\mathcal{I}_2/N \propto \beta^{-2}$. This reflects the vanishing of the classical Rényi entropy S_2 at zero temperature (see Fig. 8). The dash-dotted lines are the RS results (same as in Fig. 9). Remarkably, the RS approximation is in good agreement with the extrapolations, at least within the error bars, up to $\beta \lesssim 1.5$, whereas deviations occur at lower temperatures (not shown in the figure). For $\omega = 1/8$, the numerical results exhibit deviations from the RS result already at $\beta \gtrsim 1$. These deviations have to be attributed to the physics of the replica symmetry breaking. The full rhombi in Fig. 10 are the analytical results for $\mathcal{I}_2/N$ including some of the effects of the replica symmetry breaking. More precisely, $\mathcal{I}_2^{1\text{-}RSB}$ is obtained using Eq. (5) and the one-step replica symmetry breaking (1-RSB) approximation for the free energy of the S-K model on the booklet (cf. Eq. (42)). The agreement between $\mathcal{I}_2^{1\text{-}RSB}$ is perfect, at least up to $\beta \lesssim 2$. Notice that at lower temperatures one should expect deviations from $\mathcal{I}_2^{1\text{-}RSB}$, similar to what it is observed in the standard S-K model. In particular, one should implement the fully breaking of the replica symmetry (∞-RSB).

IX. SUMMARY AND CONCLUSIONS

We investigated the *classical* Rényi entropy S_n and the mutual information $\mathcal{I}_n$ in the Sherrington-Kirkpatrick (S-K) model, which is the paradigm model for mean-field spin glasses. As usual in disordered systems, we focused on the quenched averages $[S_n]$ and $[\mathcal{I}_n]$, with the brackets $[\cdot]$ denoting the average over different disorder realizations. Here S_n and $\mathcal{I}_n$ were obtained from suitable combinations of the partition functions of the S-K model on the so-called n-sheets booklet (cf. 1). This is obtained by "gluing" together n independent replicas ("sheets") of the model. One each replica the spins are divided into two groups A and B, containing N_A and N_B spins respectively. The spins in part A of the different sheets are identified. Due to the mean-field nature of the model, the Rényi entropies and other physical quantities depend on the bipartition only through the aspect ratio $\omega \equiv N_A/N$. Although many of our analytic results are for generic n, we often restricted ourselves to the 2-sheets booklet, i.e., the second Rényi entropy S_2 and $\mathcal{I}_2$.

We investigated the phase diagram of the S-K model on the 2-sheets booklet as a function of ω and the inverse temperature β, in the situation without external magnetic field ($h = 0$ in Eq. (1)). For any ω, in the thermodynamic limit the S-K model exhibit glassy phase for low-enough tempereatures, whereas at high temperature the model is paramagnetic. The two phases are divided by a second order phase transition, as in the standard, i.e., on the plane, S-K model. Interestingly, we found that the critical temperature depends in a non-trivial way on ω. Moreover, we fully characterized the high-temperature phase using the replica-symmetric (RS) approximation, which is a simple generalization of the replica-symmetric solution of the S-K model model on the plane. Specifically, we provided the exact formula for the disorder-averaged free energy $[F_{para}(\omega, n, \beta)]$ of the S-K model on the booklet (cf. Eq. (31)). The analytic results for S_2 and $\mathcal{I}_2$ follow straightforwardly using Eq. (7) and Eq. (5). In the low-temperature glassy phase the replica symmetry has to be broken, similar to the standard S-K model. In order to take into account the replica symmetry breaking we device a simple generalization of the the Parisi ansatz[22], which allows to break the replica symmetry in successive steps. After restricting ourselves to the one-step replica symmetry breaking, we provide the exact formula for the disorder-averaged free energy $F_{1\text{-}RSB}(\omega, n, \beta)$ (cf. Eq. (42)), and, correspondingly, S_2^{1RSB}, $\mathcal{I}_2^{1\text{-}RSB}$. As a preliminary check, we compared the analytical results for the internal energy U_{RS} and $U_{1\text{-}RSB}$ with Monte Carlo data. In the high-temperature region, where the replica symmetry is not broken, these are in perfect agreement with U_{RS}. Oppositely, in the glassy phase, where the replica symmetry breaking occurs, the Monte Carlo data exhibit deviations from the analytical results already at $\beta \approx 1$. However, we numerically observed that the one-step replica-symmetry-broken approximation $U_{1\text{-}RSB}$ matches the Monte Carlo data up to $\beta \approx 3$.

Finally, we discussed the behavior of S_2 and $\mathcal{I}_2$. Due to the mean-field nature of the S-K model we observed that both quantities obey a volume law $S_2 \propto N, \mathcal{I}_2 \propto N$. Thus we considered the densities S_2/N and $\mathcal{I}_2/N$, focusing on the thermodynamic limit $N \to \infty$, at fixed ω. At high temperature the Monte Carlo data for S_2/N are in excellent agreement with the replica-symmetric result S_2^{RS}. Interestingly, we observed that S_2/N exhibits a maximum at infinite temperature, and it is a *smooth* monotonically descreasing function of the temperature. This behavior does not depend on the booklet aspect ratio ω. Moreover, while in the high-temperature region

S_2 is fully described by the replica symmetric ansatz S_2^{RS}, in the glassy phase it exhibits signatures of the replica symmetry breaking. The one-step replica symmetry breaking approximation $S_2^{1\text{-}RSB}$ is in full agreement with the Monte Carlo data for $\beta \approx 3$, reflecting the behavior of the internal energy. Finally, we numerically observed that the mutual information per spin $\mathcal{I}_2/N$ does not show any crossing for different system sizes N, in contrast with local models, where it exhibits a crossing at the critical point. In the thermodynamic limit $\mathcal{I}_2/N$ is vanishing both at $\beta = 0$, and $\beta = \infty$, whereas it has a mximum at intermediate temperatures. The position of this maximum is not simply related to the paramagnetic glassy transition of the S-K model.

Finally, our work opens several interesting research directions. First, it would be interesting to extend our results taking into account the full breaking of the replica symmetry. This would allow to reach a conclusion on the correctness of the replica symmetry breaking scheme that we used. Moreover, it would be interesting to go beyond the saddle point approximation, including finite-size correztions. An interesting question would be to investigate hwo the paramagnetic-glassy transition is associated with the subleading corrections to the observed volume law in the classical Rényi entropies. Also, it would be interesting to investigate the behavior of entanglement-related quantities in disordered quantum spin systems that exhibit replica symmetry breaking[39,40]. Finally, it would be enlightening to understand the interplay between the physical and the fictitious replicas at the level of the entropy. Notice that, using the analytical results provided in the paper, it is possible to perform the analytic continuation $n \to 1$ to obtain the von Neumann classical mutual information. It would be interesting to check wheather this differs significantly from the Rényi mutual information.

X. ACKNOWLEDGEMENTS

We would like to thank Pasquale Calabrese for useful discussions. V.A. acknowledge financial support by the ERC under Starting Grant 279391 EDEQS.

Appendix A: The saddle point equations

In this section we provide the analytical expression for the saddle point equations (24), which determine the overlap tensor $q^{rr'}_{\gamma\gamma'}$ (see section 15) in the thermodynamic limit, and the behavior of the S-K model on the booklet. We restrict ourselves to the situation with zero magnetic field and to the 2-sheets booklet (see Fig. 1). It is straightforward to generalize the calculation to the case with non zero magnetic field and to the n-sheets booklet. Here we provide the saddle point equations obtained in both the replica-symmmetric (RS) approximation (see section IV B), and the one-step replica symmetry breaking (1-RSB) approximation (see section V).

1. The replica symmetric (RS) approximation

In the replica-symmetric approximation $q^{rr'}_{\gamma\gamma'}$ depends on the two parameters $q_0, q_0' \in \mathbb{R}$ (cf. Eq. (33)). The saddle point equations are easily derived using the RS approximation for the free energy $[F_{RS}(\omega, n, \beta)]$ (cf. Eq. (34)) of the S-K model on the booklet as $\nabla_{\mathbf{q}}[F_{RS}(\omega, 2, \beta)] = 0$, where $\mathbf{q} \equiv (q_0, q_0')$, and $\nabla_{\mathbf{q}} \equiv \partial/\partial\mathbf{q}$. A straightforward calculation gives the system of equations

$$\frac{1-q_0}{1-\omega} = 2\int dz G_0(z)(1+\exp(2\beta^2(q_0-q_0'))\cosh(2z))^{-1}, \tag{A1}$$

and

$$\begin{aligned} 2\beta^2\frac{1-q_0'}{1-\omega} = \int dz G_0(z)\Big\{ &\frac{\omega}{1-\omega}\Delta_0(z)\log\cosh(2z) \\ &+ \Delta_0(z)\log(1+\exp(2\beta^2(q_0-q_0'))\cosh(2z)) \\ &+ 2\beta^2(1+\exp(2\beta^2(q_0-q_0'))\cosh(2z))^{-1}\Big\} \end{aligned} \tag{A2}$$

where we defined $\Delta_0(z)$ as

$$\Delta_0(z) \equiv \frac{z^2}{2\beta^2 q_0'^2} - \frac{1}{2q_0'}, \tag{A3}$$

and the so-called heat kernel $G_0(z)$ as

$$G_0(z) \equiv \frac{1}{\sqrt{2\pi\beta^2 q_0'}}\exp\Big(-\frac{z^2}{2\beta^2 q_0'}\Big). \tag{A4}$$

Notice that it is trivial to check that $\int dz G_0(z)\Delta_0(z) = 0$.

2. The one-step replica symmetry breaking (1-RSB) approximation

In the one-step replica symmetry breaking scenario (see section V) the overlap depends on the four parameters $q_0, q_0', q_1', m_1 \in \mathbb{R}$. The saddle point equations are now given as $\nabla_{\mathbf{p}}[F_{1\text{-}RSB}] = 0$, where now $\mathbf{p} \equiv (q_0, q_0', q_1', m_1)$, and $[F_{1\text{-}RSB}]$ is the disorder-averaged free energy given in Eq. (42). It is useful to define the modified heat kernel $G_1(z)$ as

$$G_1(z) \equiv \frac{1}{\sqrt{2\pi\beta^2(q_1'-q_0')}}\exp\Big(-\frac{z^2}{2\beta^2(q_1'-q_0')}\Big), \tag{A5}$$

and

$$\begin{aligned} &\Delta_1(z) \equiv \frac{z^2}{\beta^2(q_1'-q_0')^2} - \frac{1}{q_1'-q_0'} \\ &\Gamma(z) \equiv \Big\{\int dz' G_1(z')\cosh^{m_1}(2z+2z')\Big\}^{-1} \\ &\Gamma'(z) \equiv \Big\{\int dz' G_1(z')\Big(1+\cosh(2z+2z')\Big)^{m_1}\Big\}^{-1} \\ &\Theta(z,z') \equiv 1+\exp(2\beta^2(q_0-q_1'))\cosh(2z+2z'). \end{aligned} \tag{A6}$$

Finally, a straightforward calculation yields the saddle point equations for q_0, q_0', q_1', m_1 as

$$0 \;=\; (1 \,+\, q_0 \,-\, 2\omega)\exp(-2\beta^2(q_0 \,-\, q_1')) \,-\, 2(1 \,-\, \omega)\int dzdz' G_0(z)\Gamma'(z)G_1(z')\cosh(2z \,+\, 2z')\Theta^{m_1-1}(z,z') \quad \text{(A7)}$$

$$\begin{aligned}0 = 4\beta^2 m_1 q_0' + \frac{\omega}{m_1}\int dz G_0(z)\Delta_0(z)\log\int dz' G_1(z')\cosh^{m_1}(2z+2z') \\ + \frac{1-\omega}{m_1}\int dz G_0(z)\Delta(z)\log\int dz' G_1(z')\Theta^{m_1}(z,z') - \frac{\omega}{m_1}\int dzdz' G_0(z)\Gamma(z)G_1(z')\Delta_1(z')\cosh^{m_1}(2z+2z') \\ - \frac{1-\omega}{m_1}\int dzdz' G_0(z)\Gamma'(z)G_1(z')\Delta_1(z')\Theta^{m_1}(z,z') \quad \text{(A8)}\end{aligned}$$

$$\begin{aligned}0 = -4\beta^2(m_1-1)q_1' - 4\beta^2\omega + \frac{\omega}{m_1}\int dzdz' G_0(z)\Gamma(z)G_1(z')\Delta_1(z')\cosh^{m_1}(2z+2z') \\ + \frac{1-\omega}{m_1}\int dzdz' G_0(z)\Gamma'(z)G_1(z')\Big\{\Delta_1(z')\Theta^{m_1}(z,z') - 4\beta^2 m_1\exp(2\beta^2(q_0-q_1'))\cosh(2z+2z')\Theta^{m_1-1}(z,z')\Big\} \quad \text{(A9)}\end{aligned}$$

$$\begin{aligned}0 = -\beta^2(q_1'^2 - q_0'^2) + \frac{\omega}{m_1}\int dzdz' G_0(z)\Gamma(z)G_1(z')\cosh^{m_1}(2z+2z')\log\cosh(2z+2z') \\ + \frac{1-\omega}{m_1}\int dzdz' G_0(z)\Gamma'(z)G_1(z')\Theta^{m_1}(z,z')\log(\Theta(z,z')) - \frac{1-\omega}{m_1^2}\int dz G_0(z)\log\int dz' G_1(z')\Theta^{m_1}(z,z') \\ - \frac{\omega}{m_1^2}\int dz G_0(z)\log\int dz' G_1(z')\cosh^{m_1}(2z+2z'). \quad \text{(A10)}\end{aligned}$$

[1] L. Amico, R. Fazio, A. Osterloh, and V. Vedral, Entanglement in Many-Body Systems, Rev. Mod. Phys. **80**, 517 (2008).

[2] J. Eisert, M. Cramer, and M. B. Plenio, Area laws for the entanglement entropy - a review, Rev. Mod. Phys. **82**, 277 (2009).

[3] P. Calabrese, J. Cardy, and B. Doyon Eds., Special issue: Entanglement entropy in extended systems, J. Phys. A **42**, 50 (2009).

[4] P. Calabrese and J. Cardy, Entanglement entropy and conformal field theory, J. Phys. A **42** 504005 (2009).

[5] C. Holzhey, F. Larsen, and F. Wilczek, Geometric and Renormalized Entropy in Conformal Field Theory, Nucl. Phys. B **424**, 443 (1994).

[6] G. Vidal, J. I. Latorre, E. Rico, and A. Kitaev, Entanglement in quantum critical phenomena, Phys. Rev. Lett. **90**, 227902 (2003). J. I. Latorre, E. Rico, and G. Vidal, Ground state entanglement in quantum spin chains, Quant. Inf. and Comp. **4**, 048 (2004).

[7] P. Calabrese and J. Cardy, Entanglement entropy and quantum field theory, J. Stat. Mech. (2004) P06002. P. Calabrese and J. Cardy, Entanglement entropy and quantum field theory: a non-technical introduction, Int. J. Quant. Inf. **4**, 429 (2006).

[8] K. Binder and A. P. Young, Rev. Mod. Phys. **58**, 801 (1986).

[9] A. P. Young, *Spin Glasses and Random Fields* (Singapore: World Scientific).

[10] J. Wilms, M. Troyer, and F. Verstraete, J. Stat. Mech. (2011) P10011.

[11] J. Wilms, J. Vidal, F. Verstraete,and S. Dusuel, J. Stat. Mech. (2012)P01023.

[12] M. Mezard, G. Parisi, and M. Virasoro, *Spin Glass theory and beyond*, World Scientific, Singapore (1987).

[13] D. S. Fisher and D. A. Huse, Phys. Rev. Lett. **56** 1601 (1986).

[14] D. S. Fisher and D. A.Huse, J. Phys. A: Math. Gen. **20** L997 (1987).

[15] D. A. Huse and D. S. Fisher, J. Phys. A: Math. Gen. **20** L1005 (1987).

[16] D. S. Fisher and D. A.Huse, Phys. Rev. B **38**, 386 (1988).

[17] C. Newman and D. L. Stein, Phys. Rev. Lett. **76**, 515 (1996).

[18] F. Krzakala and O. C. Martin, Phys. Rev. Lett. **85**, 3013 (2000).

[19] M. Palassini and A. P. Young, Phys. Rev. Lett. **85**, 3017 (2000).

[20] D. Sherrington and S. Kirkpatrick, Phys. Rev. Lett. **35**, 1972 (1978).

[21] D. Sherrington and S. Kirkpatrick, Phys. Rev. B **17**, 4385 (1978).

[22] G. Parisi, J. Phys. A **13**, 1101 (1980).

[23] G. Parisi, J. Phys. A **13**, 1887 (1980).

[24] G. Parisi, J. Phys. A **13**, L115 (1980).

[25] G. Parisi, Phys. Rev. Lett. **43**, 1754 (1979).

[26] G. Parisi, Phys. Rev. Lett **50**, 1946 (1983).

[27] M. Mezard, G. Parisi, N. Sourlas, G. Toulouse, and M. Virasoro, Phys. Rev. Lett. **52**, 1156 (1984).

[28] H. Nishimori, "Statistical Physics of Spin Glasses and Information Processing", Clarendon Press, Oxford (2001).

[29] J.-M. Stéphan, S. Inglis, P. Fendley, and R. G. Melko, Phys. Rev. Lett. **112**, 127204 (2014).

[30] J. Iaconis, S. Inglis, A. B. Kallin, and R. G. Melko, Phys. Rev. B **87**, 195134 (2013).

[31] B. Yucesoy, H. G. Katzgraber, and J. Machta, Phys. Rev. Lett. **109**, 177204 (2012).

[32] B. Yucesoy, H. G. Katzgraber, and J. Machta, Phys. Rev. Lett. **110**, 219702 (2013)

[33] A. Billoire, L. A. Fernandez, A. Maiorano, E. Marinari, V. Martin-Mayor, G. Parisi, F. Ricci-Tersenghi, J. J. Ruiz-Lorenzo, and D. Yllanes, Phys. Rev. Lett. **110**, 219701 (2013).

[34] S. Morrison, A. Kantian, A. J. Daley, H. G. Katzgraber, M. Lewenstein, H. P. Büchler, and P. Zoller, New J. Phys. **10**, 073032 (2008).

[35] N. Ghofraniha, I. Viola, F. Di Maria, G. Barbarella, G. Gigli, L. Leuzzi, and C. Conti, Nature Comm. **6**, 6058 (2015).

[36] P. Rotondo, E. Tesio, and S. Caracciolo, Phys. Rev. B **91**, 014415 (2015).

[37] T. Aspelmeier, A. Billoire, E. Marinari, and M. A. Moore, J. Phys. A: Math. Theor. **41** 324008 (2008).

[38] A. Billoire, in *Rugged Free Energy Landscape*, Springer Lecture Notes in Physics, edited by W. Janke (Springer, Berlin-Heidelberg 2007.

[39] N. Read, S. Sachdev, and J. Ye, Phys. Rev. B **52**, 384 (1995).

[40] A. Andreanov and M. Müller, Phys. Rev. Lett. **109**, 177201 (2012).

[41] J. Cardy, *Scaling and Renormalization in Statistical Physics* (Cambridge Lecture Notes in Physics).

[42] J. R. L. de Almeida and D. J. Thouless, J. Phys. A **11**, 983 (1978).

[43] J-M Stéphan, S. Furukawa, G. Misguich, and V. Pasquier, Phys. Rev. B, **80**, 184421 (2009)

[44] J-M Stéphan, G. Misguich, and V. Pasquier, Phys. Rev. B, **82**, 125455 (2010);

[45] J-M Stéphan, G. Misguich, and V. Pasquier, Phys. Rev. B **84**, 195128 (2011).

[46] M. P. Zaletel, J. H. Bardarson, and J. E. Moore, Phys. Rev. Lett. **107**, 020402 (2011).

[47] F. C. Alcaraz and M. A. Rajabpour, Phys. Rev. Lett. **111**, 017201 (2013).

[48] M. Talagrand, Ann. of Math. **163**, 221 (2006).

[49] F. Guerra and F. L. Toninelli, Commun. Math. Phys. **230**, 71 (2002).

[50] R. Rammal, G. Toulouse, and M. A. Virasoro, Rev. Mod. Phys. **58**, 765 (1986).

[51] P. Calabrese, J. Cardy, and E. Tonni, Phys. Rev. Lett. **109**, 130502 (2012).

[52] J.-M. Stéphan, Phys. Rev. B **90**, 045424 (2014).

[53] T. Castellani and A. Cavagna, J. Stat. Mech. (2005) P05012.

[54] M. M. Wolf, F. Verstraete, M. B. Hastings, and J. I. Cirac, Phys. Rev. Lett. **100**, 070502 (2008).

[55] G. Refael and J. E. Moore J. Phys. A: Math. Theor. **42** 504010 (2009).

[56] L. A. Pastur and M. V. Shcherbina, J. Stat. Phys. **62**, 1 (1991).